

S₋₃ State of the Water Oxidase in Photosystem II[†]

J. Messinger,* G. Seaton, and T. Wydrzynski

*Photobioenergetics, Research School of Biological Sciences, The Australian National University,
P.O. Box 475, ACT 2601, Australia*

U. Wacker and G. Renger

Max Volmer Institut, Technische Universität Berlin, Strasse des 17. Juni 135, D 10623 Berlin, Germany

Received October 23, 1996; Revised Manuscript Received March 19, 1997[®]

ABSTRACT: The effect of the reductant hydrazine on the flash-induced oxygen oscillation patterns of spinach thylakoids was used to characterize a new super-reduced redox state of the water oxidase in photosystem II. The formation of a discrete S₋₃ state is evident from the shift of the first maximum of oxygen evolution from the 3rd flash through the 5th flash to the 7th flash during a 90 min incubation of dark-adapted thylakoids with 10 mM hydrazine sulfate at pH 6.8 on ice. A distinct period four oscillation with further maxima on the 11th and 15th flashes is still observed at this stage of the incubation. The data analysis within the framework of an extended Kok model reveals that a S₋₃ state population of almost 50% can be achieved by this treatment. A prolonged incubation of the S₋₃ sample with 10 mM hydrazine (and even 100 mM) does not lead to a further shift of the first maximum toward the 9th flash that could reflect the formation of the S₋₅ state. Instead, a slow oxidation of S₋₃ to S₋₂ takes place by an as yet unidentified electron acceptor. A consistent simulation of all the measured oxygen oscillation patterns of this study could, however, only be achieved by including the formal redox states S₋₄ and S₋₅ in the fits (S₋₄ + S₋₅ up to 35%). The implications of these findings for the oxidation states of the manganese in the tetranuclear cluster of the water oxidase are discussed.

Photosynthetic water oxidation to molecular oxygen in cyanobacteria and plants is catalyzed by the integral membrane chlorophyll/protein complex photosystem II (PS II).¹ Four manganese ions organized into two pairs of bis-μ-oxo bridged dimers are known to be essential for the process of water oxidation in PS II [for reviews, see e.g. Nugent (1996), Renger (1993), Debus (1992), and Hansson and Wydrzynski (1990)]. They form (at least in part) the site for storing the oxidizing equivalents created by the light-induced charge separation between P680 and Pheo in the reaction center of PS II [for review, see Renger (1992)] and also the catalytic site of water oxidation. Upon illumination, the water oxidase

cycles through five different redox states termed S₀–S₄ (Kok et al., 1970). This sequence of four univalent oxidation steps was deduced from the period four oscillation of flash-induced oxygen evolution patterns measured first by Joliot et al. (1969). The S_i → S_{i+1} transitions are energetically driven by the chlorophyll cation radical P680^{•+} formed during the primary charge separation with the redox active tyrosine Y_Z [tyrosine 160 (161) of polypeptide D1] acting as the intermediary electron carrier. After a thorough dark adaptation, all PS II centers are in the S₁ state, since in the dark S₂ and S₃ are reduced by internal electron donors to S₁ while S₀ is slowly oxidized to S₁ by Y_D^{ox}, the oxidized form of tyrosine 161 of the D2 protein. Molecular oxygen is formed from substrate water during the oxidation of the S₃ state by Y_Z^{ox}. For the S₂ and S₃ states of the water oxidase, it was recently shown (Messinger et al., 1995a,b) that the two substrate water molecules exchange with different rates; i.e. one exchanges fast (*k_f* ≥ 40 s⁻¹) and one more slowly (*k_s* = 2.2 s⁻¹ at 10 °C and pH 7.0).

A further redox state S_i of the water oxidase, which is not part of the Kok cycle (*i* = 0–4), was first described by Bouges (1971) and termed the S₋₁ state. She discovered that the exogenous reductant hydroxylamine can induce a two-electron shift of the first maximum of oxygen evolution from the 3rd to the 5th flash. It has been controversial for a long time whether the super-reduced S₋₁ state represents a different redox state of the manganese cluster, a reduction of another PS II donor side component, or the tight binding of the reductant to the catalytic site. In the latter case, it

[†] J.M. acknowledges the financial support of postdoctoral fellowships from the Australian Research Council (ARC) and the EC (EC HCMF). G.R. was supported by the Deutsche Forschungsgemeinschaft (DFG).

* Author to whom correspondence should be addressed: Dr. J. Messinger, Lawrence Berkeley Laboratory, Structural Biology Division, Building 3, 1 Cyclotron Road, Berkeley, CA 94720.

[®] Abstract published in *Advance ACS Abstracts*, May 1, 1997.

¹ Abbreviations: α, miss probability; β, double-hit probability; c(Chl), chlorophyll concentration; cyt_{b559}, cytochrome b₅₅₉; *d*, activity parameter; dy_i², standard deviation; EPR, electron paramagnetic resonance; EXAFS, extended X-ray absorption fine structure; fq, fit quality; PS II, photosystem II; P680 and P680^{•+}, reaction center chlorophyll of PS II and its cation radical form, respectively; Pheo, pheophytin molecule of the PS II reaction center that acts as the electron acceptor during the primary charge separation; S_i states, redox states of the water oxidase in PS II; XANES, X-ray absorption near edge spectroscopy; Y_D, redox active tyrosine of the PS II polypeptide D2, but not part of the main electron transport chain; Y_n, oxygen yield of the *n*th flash; Y_Z, redox active tyrosine of the D1 polypeptide of PS II that acts as the electron donor to P680^{•+}.

was postulated that hydroxylamine could only become oxidized by the S₂ state formed upon flash illumination and the shift was due to the rapid reaction in the dark time between the flashes of the detecting flash train. On the basis of different lines of evidence, it is now widely accepted that the exogenous reductants hydrazine and hydroxylamine can reduce the manganese ions of the water oxidase during dark incubation [for review, see Guiles et al. (1990), Brudvig and Beck (1992), and Debus (1992)]. This view is supported by the slow dark reactions that lead to the shift (Brudvig & Beck, 1992; Messinger et al., 1991b), the fact that the two-electron shift cannot be reversed by removal of hydroxylamine or hydrazine from the sample (Beck & Brudvig, 1987; Kretschmann et al., 1991; Messinger & Renger, 1993), the finding that S₋₁ can be oxidized by Y_D^{ox} to S₀ (Messinger & Renger, 1993), and Mn K-edge shifts toward lower energy observed after incubation of dark-adapted PS II core particles with hydroxylamine (Riggs et al., 1992; Riggs-Gelasco et al., 1996). The recent discovery of the even further reduced S₋₂ state also makes a pure binding model very unlikely (Renger et al., 1990; Messinger & Renger, 1990; Messinger et al., 1991a,b; Kretschmann et al., 1991).

The redox states of the four manganese ions of the water oxidase in the dark stable S₁ state are still controversial. From recent EPR S₂ state multiline signal simulations (Zheng & Dismukes, 1996), a redox state of four Mn(III) is favored for S₁, while Mn K-edge XANES measurements strongly suggest a configuration of two Mn(III) and two Mn(IV) (Ono et al., 1992; Riggs et al., 1992; Yachandra et al., 1993). On the basis of these results, the water oxidase should be able to attain states reduced even further than S₋₂. In the case of S₁ being four Mn(III), the lowest S_i state would be S₋₃, and in the latter case, it could even be S₋₅, providing that the manganese ions of the water oxidase can be reduced to Mn(II) without leaving their binding sites. Therefore, a careful redox titration of the water oxidase can produce complementary information about the redox states of the manganese ions in the dark stable S₁ state.

The existence of an unstable S₋₃ state has been discussed before (Lavergne, 1989; Beck & Brudvig, 1987; Mei & Yocum, 1991; Riggs-Gelasco et al., 1996) but was discounted by Kretschmann and Witt (1993). Some indirect evidence for a S₋₃ state in PS II has been reported previously, on the basis of the analysis of oxygen oscillation patterns of spinach thylakoids which had been incubated with 50–250 μM hydroxylamine or 1 mM hydrazine (Messinger et al., 1991b; Kebekus et al., 1995). In these studies, the maximal S₋₃ population never exceeded 20% and, therefore, no firm conclusions could be drawn. The present study provides evidence for the existence of a discrete and relatively stable S₋₃ state in spinach thylakoids that were suitably treated with high hydrazine concentrations (10 and 100 mM). This finding supports conclusions that in the S₁ state the average oxidation state of the four manganese ions in the water oxidase is at least Mn(III).

MATERIALS AND METHODS

Thylakoids were prepared in dim green light from freshly picked, hydroponically grown spinach using a buffer containing 400 mM sucrose, 15 mM NaCl, 5 mM MgCl₂, and 50 mM Hepes/NaOH at pH 7.0 and 4 °C as described in Messinger et al. (1995b). The chloroplast envelopes were

broken in a homogenizer, as this seemed to increase the stability of the reduced S_i states compared to those of samples prepared by using an osmotic shock treatment. The thylakoids [*c*(Chl) = 3 mg/mL] were frozen in liquid nitrogen as small beads and stored at -80 °C until used.

Before the measurements, the samples were thawed in the dark on ice and diluted to a *c*(Chl) of 1.25 mg/mL with ice cold buffer A containing 400 mM mannitol, 20 mM CaCl₂, 10 mM MgCl₂, and 50 mM Hepes/NaOH at pH 6.8 and 2 °C. At the start of an incubation, they were further diluted to a *c*(Chl) of 1 mg/mL either with buffer A (control samples) or with hydrazine sulfate (N₂H₆SO₄, Fluka, >99.0%) dissolved in buffer A. The hydrazine solutions were prepared, and the pH was adjusted (pH 6.8 and 2 °C) shortly before the start of incubation. The hydrazine incubation was performed in the dark on ice. At different times during the incubation, 15 μL aliquots were taken in very dim green light (LED lamp) and rapidly transferred to the bare platinum cathode of the Joliot type electrode (see below). The polarization of -750 mV (against the Ag/AgCl anode) was switched on about 30 s before the first flash, which is the minimum time required to achieve a constant potential in our setup. The total time for sample transfer and measurement was about 1 min.

The oxygen oscillation patterns were measured with a home-built (Research School of Biological Sciences, The Australian National University) unmodulated Joliot type electrode (Joliot, 1972; Messinger, 1993) that keeps the temperature of the electrode and the buffer reservoir constant within ±0.3 °C. For flash excitation, a xenon flash lamp (EG&G, 4 μF, 1 kV capacitor) was used that was triggered from a personal computer. The flash-induced amperometric signals were uncoupled from the steady background signal caused by oxygen dissolved in the flow buffer (buffer A at pH 6.8 and 10 °C) using an isolation transformer. The isolated and amplified signals were then digitized with an A/D board and stored in a personal computer. The sampling rate was 1 point/ms, and a total of 16 flashes at a rate of 2 Hz were recorded. The first flash was given 200 ms after the start of data recording.

The data were analyzed within the framework of an extended Kok model essentially as described earlier (Messinger et al., 1991b; Kebekus et al., 1995). The fit program was based on the formulas

$$S_n = \mathbf{K} S_{n-1} d \quad (1)$$

and

$$Y_n = (1 - \alpha)[S_3]_{n-1} + \beta[S_2]_{n-1} \quad (2)$$

where S_{n-1} and S_n are vectors of the S_i state populations before and after the *n*th flash of the train, \mathbf{K} is the matrix containing the Kok parameters α (miss probability), β (double-hit probability), $\gamma = 1 - \alpha - \beta$ (single-hit probability), and 0 (no transition occurs; for details, see Messinger et al. (1991b)), *d* is an activity parameter that compensates for an increase or decrease in the number of active PS II centers during the flash train [this parameter is similar in intention but not identical to the *z* parameter introduced by Delrieu and Rosengard (1987) and used later by Meunier and Popovic (1991), as *d* is an independent parameter, while *z* is linked to the miss, double- and single-

hit probabilities by the equation $z = \alpha + \beta + \gamma$, Y_n is the oxygen yield due to the n th flash, and $[S_3]_{n-1}$ and $[S_2]_{n-1}$ are the normalized S_3 and S_2 state populations immediately before the n th flash, respectively. The S_i state vectors used here were extended to also contain the S_{-1} – S_{-5} states. Correspondingly, the Kok matrix \mathbf{K} was extended using the same miss and double-hit probabilities for all $S_i \rightarrow S_{i+1}$ state transitions.

In order to analyze the possibility of two-electron reductions of the S_i states during the dark time of 500 ms between the flashes due to reactions with hydrazine, the following differential equations were used to calculate numerically the resulting redistributions between the individual flashes (an iteration step with dt of 0.5 ms was used):

$$d[S_3]/dt = -k_{3,1}[S_3]$$

$$d[S_2]/dt = -k_{2,0}[S_2]$$

$$d[S_1]/dt = -k_{1,-1}[S_1] + k_{3,1}[S_3]$$

$$d[S_0]/dt = -k_{0,-2}[S_0] + k_{2,0}[S_2]$$

$$d[S_{-1}]/dt = -k_{-1,-3}[S_{-1}] + k_{1,-1}[S_1]$$

$$d[S_{-2}]/dt = k_{0,-2}[S_0]$$

$$d[S_{-3}]/dt = k_{-1,-3}[S_{-1}]$$

where $k_{i,i-2}$ are the first-order rate constants for the reaction $S_i \rightarrow S_{i-2}$. No reactions leading to S_{-4} or S_{-5} have been taken into account, as the above reduction reactions have only been considered in attempts of data fits that exclude the existence of S_{-4} and S_{-5} .

All parameters were varied manually according to different fit strategies explained in Results. Thereby, the number of free parameters for the individual fits was reduced from 13 to usually 5 to 8 (see figure legends and tables). The standard deviations were calculated as follows:

$$dy_i^2 = \sum (y_n^{\text{fit}} - y_n^{\text{exp}})^2 \quad (3)$$

where $y_n^{\text{fit}} = Y_n^{\text{fit}}/\sum Y_n^{\text{fit}}$ and $y_n^{\text{exp}} = Y_n^{\text{exp}}/\sum Y_n^{\text{exp}}$ are the normalized values (yield of the n th flash normalized to the sum of all considered flashes) of the calculated and measured oxygen yields, respectively. In order to compare fits with different numbers of data points or free parameters, the fit quality (fq) was calculated from this expression as follows:

$$\text{fq} = dy_i^2/(F - P) \quad (4)$$

where F is the number of flashes (i.e. data points) used for the fit and P is the number of free parameters.

The initial S_i state populations were normalized according to

$$\sum_{i=-5}^3 [S_i] = 1 \quad (5)$$

RESULTS

Formation of the S_{-3} State. Oxygen oscillation patterns of spinach thylakoids were measured with a Joliot type electrode at 10 °C and pH 6.8 using a flash frequency of 2

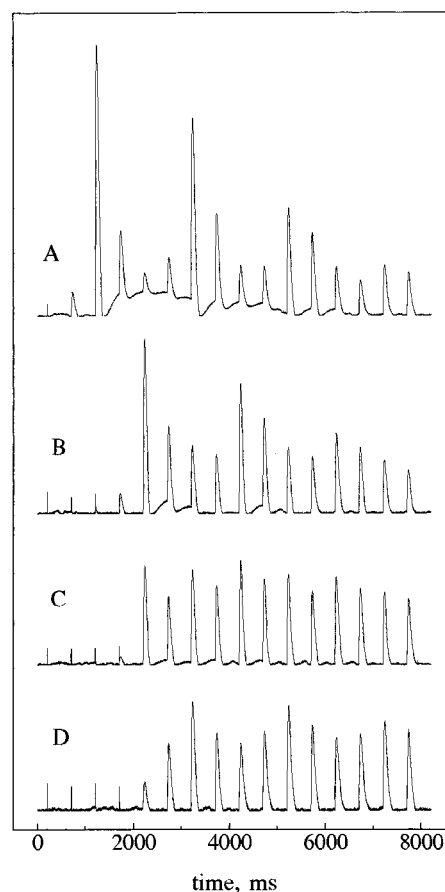


FIGURE 1: Oxygen oscillation patterns of dark-adapted spinach thylakoids induced by a train of saturating xenon flashes (2 Hz) measured with a Joliot type electrode at 10 °C and pH 6.8. Before the measurement, the thylakoids were incubated in the dark at a chlorophyll concentration of 1 mg/mL on ice for different times with 10 mM $\text{N}_2\text{H}_4\text{SO}_4$ in a buffer containing 400 mM mannitol, 20 mM CaCl_2 , 10 mM MgCl_2 , and 50 mM Hepes/NaOH (pH 6.8 and 2 °C). The aliquots were taken either before (A) or 5 min (B), 30 min (C), or 90 min (D) after the addition of hydrazine. Sharp spikes indicate small flash artifacts (first flash at 200 ms). All patterns are normalized so they have an identical sum over the oxygen yields due to flashes 7–10.

Hz. Figures 1 and 2 depict original traces obtained after different times of incubation with 10 mM hydrazine. In general, three types of signals can be observed: (1) small, very short (1–2 ms) spikes of approximately the same height, (2) somewhat broader signals (approximately 100 ms), which oscillate in size, and (3) very broad (500–2000 ms) baseline signals. The spikes are due to small flash artifacts and do not represent oxygen evolution. No special efforts were made to completely avoid these artifacts, as they do not interfere with the oxygen signals and are convenient indicators for the flash excitations. The amplitude of the rise of the type 2 signals is proportional to the amount of oxygen induced by the respective flash in the thylakoids. In contrast, the broad baseline signals, which usually occur after large oxygen signals, are simply due to “electronic swinging” of the isolation transformer circuit used to uncouple the flash-induced oxygen signals from the steady state signals caused by oxygen dissolved in the flow buffer. In some cases, the decay of the oxygen signals is apparently truncated as a DC restorer circuit has been used to prevent the signals from going below zero. In order to visualize the specific changes (i.e. those which are not due to inactivation of part of the centers) in the flash-induced oxygen yields induced by

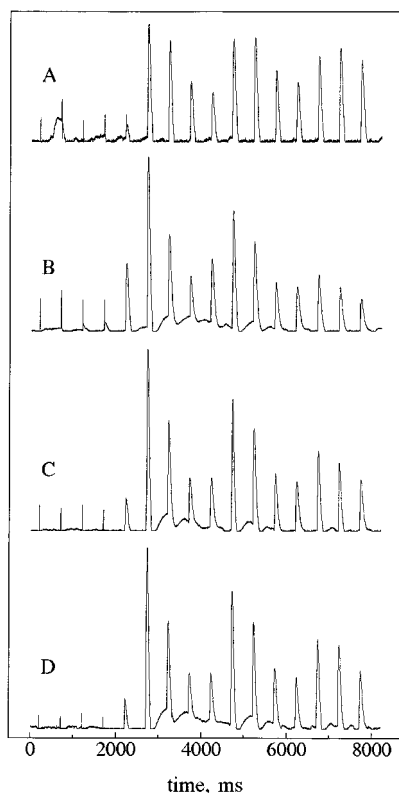


FIGURE 2: Oxygen oscillation patterns of spinach thylakoids after different times of incubation with 10 mM NH_2NH_2 on ice (A) after 5 h of incubation of S_1 thylakoids. Patterns B–D were obtained from aliquots of a sample that was first incubated for 5 min with 10 mM hydrazine to give a high S_{-1} population (see Figure 1B) and was then mostly converted into the S_0 state by the illumination with one saturating xenon flash outside the Joliot electrode. This was followed by a further incubation in the dark on ice for 5 min (B), 90 min (C), and 180 min (D). All other conditions were as described in Figure 1.

hydrazine incubation, all traces were normalized to have the same sum of oxygen yields for flashes 7–10. This method was chosen, because the oxygen yields of flashes 7–10 are (i) almost invariant to the hydrazine-induced backward shifts of oxygen yields and (ii) only marginally effected by the relative increase of oxygen yields at higher flash numbers, which is a consequence of the inactivation of other PS II centers (see below).

Figure 1A shows a typical oxygen oscillation pattern of dark-adapted spinach thylakoids with the first maximum in the 3rd flash and further maxima in the 7th, 11th, and 15th flashes. On the basis of the Kok model (Kok et al., 1970), the pronounced oscillations show a very high initial S_1 state population and low miss (α) and double-hit (β) probabilities (see below). A closer inspection of this pattern reveals that the overall oxygen yield progressively declines with increasing flash number, especially after the 10th flash. This feature is due to the limited number of plastoquinone molecules per PS II complex, i.e. the limited electron acceptor pool capacity in the absence of an exogenous electron acceptor. This strong decay is typical for highly intact thylakoids measured under these temperature conditions (10 °C) which prevent an efficient reoxidation of the plastoquinone molecules between flashes (Messinger et al., 1993).

Panels B–D of Figure 1 show oxygen oscillation patterns of spinach thylakoids that were dark incubated for different times with 10 mM hydrazine sulfate at pH 6.8 on ice. An

almost complete shift of the first maximum to the 5th flash is already observed with an aliquot measured after 5 min (Figure 1B). This two-electron reduction by hydrazine has been described earlier [for a review, see Debus (1992)] and shows the formation of the S_{-1} state in the water oxidase. After 30 min of dark incubation (Figure 1C), a further two-electron shift starts to become obvious from a binary oscillation with about equal oxygen yields in the 5th, 7th, and 11th flashes. After 90 min, the oxygen yield owing to the 5th flash is rather small and the first maximum of the pattern is shifted to the 7th flash. A clear period four oscillation is still discernible under these conditions with further maxima in the 11th and 15th flashes (Figure 1D). This indicates that no significant increase of the miss parameter occurs during the 90 min dark incubation time, although the overall oxygen flash yield declines by about 50% over this time period (data not shown). The striking four-flash delay of the first maximum shows that in a significant fraction of active photosystem II centers the water oxidase attains an overall electronic configuration which contains a surplus of four electrons compared to the S_1 state. Therefore, in the following, this state will be referred to as the S_{-3} state of the water oxidase.

During the 90 min incubation with hydrazine, a rise in the “steady state” oxygen yields, i.e. in the yields of flashes 11–16 relative to the yields of flashes 7–10, is observed. This phenomenon reflects the hydrazine-induced inactivation of about half of the PS II centers during this time period which doubles the relative size of the plastoquinone pool for those centers which remain active. A similar phenomenon was observed in PS II membrane fragments when part of the PS II centers was inhibited by DCMU (Renger et al., 1989).

A prolonged incubation under the above conditions gives rise to a slow increase in the oxygen yield of the 6th flash. An oscillation pattern obtained from thylakoids after a 5 h dark incubation with 10 mM hydrazine is shown in Figure 2A (the broad feature between the 1st and 2nd flash is a baseline artifact). This one-electron shift can be ascribed to a slow dark oxidation of the S_{-3} state to the S_{-2} state. Remarkably, no further shift of the first maximum toward the 9th flash was observed that could indicate the formation of the S_{-5} state.

In order to analyze these phenomena in more detail, normalized oxygen yields of the 5th (solid triangles, Y_5), 6th (open diamonds, Y_6), and 7th (open inverted triangles, Y_7) flashes were measured as a function of the incubation time with 10 mM hydrazine within a time domain of up to 150 min (Figure 3A). The decay of Y_5 can be fitted (solid line) with an apparent first-order rate constant of approximately 0.028 min^{-1} . The oxygen yield of Y_7 increases with the same rate, but the total extent of this rise is markedly smaller. The amplitude of Y_6 declines first with Y_5 but rises then slowly because of the oxidation of S_{-3} to S_{-2} (see Discussion).

Attempts to Form the Redox States S_{-4} and S_{-5} . In order to check whether this high hydrazine concentration, which is 10 times higher than that previously used (Messinger et al., 1991; Messinger & Renger, 1993), additionally leads to a two-electron reduction of S_{-2} to S_{-4} , another batch of thylakoids was first incubated for 5 min with 10 mM hydrazine to achieve a high S_{-1} population (see Figure 1B) and then illuminated with one saturating xenon flash, which converts most of the PS II centers into the S_0 state.

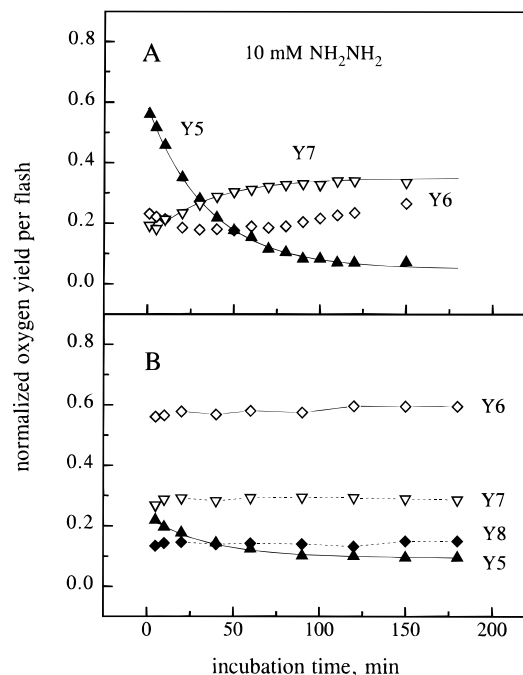


FIGURE 3: Normalized oxygen yields due to flashes 5 (Y_5 , solid triangles), 6 (Y_6 , open diamonds), 7 (Y_7 , inverted open triangles), and 8 (Y_8 , solid diamonds) as a function of dark incubation time on ice with 10 mM NH_2NH_2 at pH 6.8: (A) starting with dark-adapted S_1 thylakoids and (B) starting with a high S_0 state concentration which was obtained by a 5 min incubation of S_1 thylakoids with 10 mM NH_2NH_2 and one saturating xenon flash. Symbols are the experimental values. The solid lines in panel A were obtained by simple first-order fits, while all other lines in panels A and B simply connect the data points for the sake of clarity.

Thereafter, the sample was further incubated on ice, and flash-induced oxygen oscillation patterns were measured at different times after the S_0 state formation. The results depicted in Figure 2B reveal that after 5 min of incubation S_0 has been almost completely reduced by hydrazine to S_{-2} as reflected by the small oxygen yield in the 4th and the pronounced first maximum in the 6th flash (Messinger & Renger, 1990; Messinger et al., 1991b). The results of panels C (90 min) and D (180 min) of Figure 2 show that a drastic extension of the dark incubation of the sample gives rise to only minor changes in the oxygen oscillation patterns, which can be ascribed to the reduction of the S_{-1} state (Y_5) to S_{-3} (Y_7) and its reoxidation to S_{-2} (Y_6) (see also Figure 3B). It is obvious that a pronounced shift of the first maximum to the 8th flash does not occur, i.e. that no significant S_{-4} formation can be achieved under these conditions.

At a first glance, the results of Figures 1 and 2 seem to indicate that the S_{-3} state is the lowest stable oxidation state of the water oxidase in PS II. However, the lack of a significant population of S_{-4} and S_{-5} might be simply due to very slow reduction rates of S_{-2} and S_{-3} . The idea of a kinetic limitation can be checked by a marked increase of the hydrazine concentration because the rate of S_i state reduction was found to exhibit a linear dependence on the concentration of reductant for an i of 0–3 (Messinger et al., 1991b). A similar effect is expected for S_{-2} and S_{-3} . Therefore, experiments were performed at a 10-fold hydrazine concentration (100 mM) and at incubation times of up to 60 min. The reaction starting from S_0 was achieved at this concentration by giving one flash at 1 min after the start of incubation. The results obtained are depicted in panels

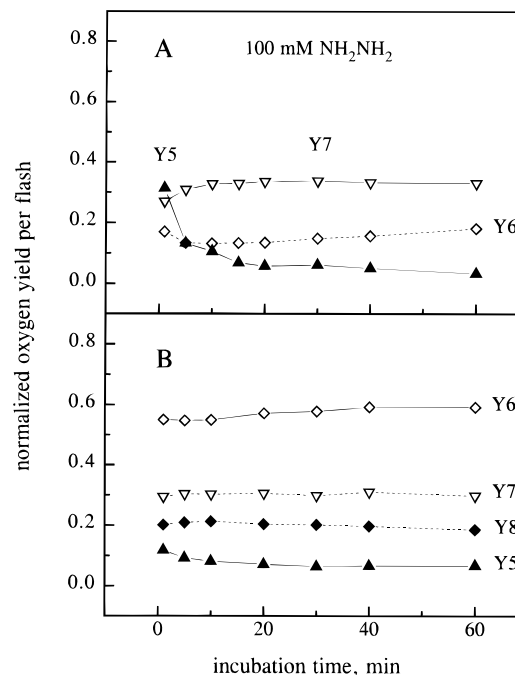


FIGURE 4: Normalized oxygen yields due to flashes 5 (Y_5 , solid triangles), 6 (Y_6 , open diamonds), 7 (Y_7 , inverted open triangles), and 8 (Y_8 , solid diamonds) as a function of dark incubation time on ice with 100 mM NH_2NH_2 at pH 6.8: (A) starting with dark-adapted thylakoids (S_1 state) and (B) starting with a high S_0 state population, which was obtained by incubating S_1 thylakoids for 1 min with 100 mM hydrazine and then giving one saturating xenon flash. Symbols are the experimental values, and the lines simply connect the data points for the sake of clarity.

A (reaction starting at S_1) and B (reaction starting at S_0) of Figure 4. Except for the expected faster reduction rates of S_1 , S_{-1} , and S_0 , qualitatively very similar results were obtained as in the case of 10 mM hydrazine (Figure 3A,B). Again, no shift of the first maximum toward the 9th (Figure 4A shows no decline in Y_7) or 8th (Figure 4B) flash and therefore no hydrazine-induced S_{-5} or S_{-4} formation can be seen. This finding seems to rule out kinetic limitations for the inability of hydrazine to reduce S_{-3} and S_{-2} under these conditions. Nevertheless, a closer inspection of the data reveals that the oxygen yield of the 8th flash is higher in the data set gathered from experiments with 100 mM hydrazine than in the case of 10 mM hydrazine (for a comparison, see Y_8 in Figures 3B and 4B). Analogously, the oxygen yield of the 9th flash is slightly higher for S_1 thylakoids after a 100 mM hydrazine incubation compared with that of samples incubated at 10 mM (not shown).

Determination of the Normalized S_i State Populations within an Extended Kok Model. In order to analyze the above oxygen flash yield pattern, the Kok model was extended to also include the S_i states below S_0 down to S_{-5} (see Materials and Methods). As a convenient approximation, identical miss and double-hit probabilities have been used for all the S_i state transitions. An activity parameter, d , was introduced in order to account for changes in the number of active water oxidases during the flash train. Furthermore, the conventionally “static” Kok model was extended to a “kinetic S_i state model” that also takes into account possible hydrazine-induced two-electron reductions of the S_i states for an i of 3 to -1 during the dark time between the flashes. To reduce the number of free parameters, only the rate of the S_2 reduction ($k_{2,0}$) was fitted freely

Table 1: Comparison of Different Fit Approaches for Control Oxygen Oscillation Patterns of Dark-Adapted Thylakoids (Figure 1A)^a

fit	S ₂ (%)	S ₁ (%)	S ₀ (%)	S ₋₁ (%)	α (%)	β (%)	d	f _q	Δf _q (%)
a	—	(100)	—	—	7.9	2.5	(1.000)	0.0057	—
b	—	(100)	—	—	8.0	2.7	0.985	0.0032	44
c	—	96.5	—	3.5	7.6	2.4	0.981	0.0018	44
d	1.5	94.5	—	4.0	7.6	2.1	0.979	0.0009	50
e	1.5	93.0	2.0	3.5	7.2	2.1	0.978	0.0009	0
f	2.0	95.0	—	3.0	7.5	2.0	0.983	0.0013	—
g	2.5	94.0	—	3.5	7.4	2.0	0.981	0.0014	—
h	2.5	94.5	—	3.0	6.9	2.1	0.981	0.0011	—

^a Parameters: S₂–S₋₁, normalized S_i state populations; α, miss probability; β, double-hit probability; and d, activity parameter. The first 10 flash yields of each oscillation pattern have been used to calculate the fit quality (f_q, see Materials and Methods). Other symbols: —, parameter was excluded from the fit (set to zero). Numbers in parentheses give values which were restrained to values different from zero. Fits: 1a (2 free parameters), the initial S₁ state population was set to 100% and only α and β were varied; 1b (3 free parameters), as 1a, but in addition the activity parameter was varied; 1c (5 free parameters), as before, but the S₁ and S₋₁ state populations were also optimized; 1d (6 free parameters), as before, but also the initial S₂ state population was a free parameter; 1e (7 free parameters), as 1d, but also the S₀ state population was optimized; 1f and 1g (6 free parameters), as fit 1d, but two other measurements of the same control sample have been used for the fits; and 1h (6 free parameters), same sample as for the other fits, but the aliquot was preflashed and dark adapted again before the measurement. The relative change in fit quality (Δf_q) is always calculated with respect to the previous fit.

Table 2: Kok Parameter Used for Different Types of Simulations of Oxygen Oscillation Patterns Shown in Figures 2, 5, and 6^a

Figure	original S _i state, incubation conditions	fit	k _{2,0} (s ⁻¹)	S ₋₁ (%)	S ₋₂ (%)	S ₋₃ (%)	S ₋₄ (%)	S ₋₅ (%)	α (%)	β (%)	d	f _q
2A	S ₁ , 5 h with 10 mM NH ₂ NH ₂	a (ns)	—	0.0	54.0	29.0	11.0	6.0	(7.4)	(2.1)	1.000	0.0006
5A	S ₁ , 90 min with 10 mM NH ₂ NH ₂	b (broken)	—	27.0	73.0	—	—	—	26.0	0.7	1.040	0.0570
		c (dots)	—	13.0	28.0	59.0	—	—	12.3	2.3	1.046	0.0133
		d (ns)	0.50	13.0	31.5	55.5	—	—	9.2	(2.1)	1.025	0.0044
		e (solid)	—	9.5	23.0	44.0	13.5	10.0	(7.4)	(2.1)	1.000	0.0019
5B	S ₀ , 90 min with 10 mM NH ₂ NH ₂	f (broken)	—	92.0	8.0	—	—	—	(26.0)	(0.7)	(1.040)	0.5587
		g (dots)	—	0.0	90.5	9.5	—	—	8.0	3.4	0.992	0.0200
		h (ns)	0.14	4.5	88.5	7.0	—	—	(7.4)	(2.1)	1.000	0.0006
		i (solid)	—	3.5	80.0	7.0	8.5	1.0	(7.4)	(2.1)	0.980	0.0012
6A	S ₁ , 15 min with 100 mM NH ₂ NH ₂	j (broken)	2.50	30.0	70.0	—	—	—	(11.5)	(2.1)	1.000	0.5659
		k (dots)	0.50	12.5	13.5	74.0	—	—	11.5	(2.1)	1.000	0.0047
		l (solid)	—	7.5	10.5	47.5	17.0	17.5	(7.4)	(2.1)	0.970	0.0034
6B	S ₀ , 10 min with 100 mM NH ₂ NH ₂	m (dots)	0.50	0.5	86.5	13.0	—	—	(7.4)	(2.1)	0.955	0.0010
		n (solid)	—	0.5	64.5	10.0	21.0	4.0	(7.4)	(2.1)	0.910	0.0008

^a Parameters of the extended Kok model (see Materials and Methods): S₋₅–S₋₁, normalized S_i state populations; and k_{2,0}, rate constant for the reaction of NH₂NH₂ with the S₂ state during the dark time between the flashes. The rates for the two-electron reductions of the other S_i states can be obtained from the following ratios: k_{2,0}/k_{0,-2} = 4; k_{2,0}/k_{1,-1} = 8; k_{2,0}/k_{3,1} = 16; k_{2,0}/k_{-1,-3} = 80 [see Messinger et al. (1991) and this study]. Other parameters: α, miss probability; β, double-hit probability; and d, activity parameter. The first 10 flash yields of each oscillation pattern have been used to calculate dy_i² (standard deviation) and the fit quality (f_q, see Materials and Methods). As no oxygen yields are observed before the 5th flash in any of these patterns, the initial S₃ and S₂ state populations were fixed to zero and were not counted as free parameters, while for reasons of better comparison with Table 4, the S₁ and S₀ state populations (also zero and not shown in this table) were always counted as free parameters. Other symbols: —, parameter was excluded from the fit (set to zero). Numbers in parentheses give values which were restrained to values different from zero; the value for the most populated S_i state in each fit is printed in bold.

Table 3: Fits of the Oxygen Oscillation Pattern Obtained after 90 min of Incubation with 10 mM Hydrazine (Figure 1D) Using All 16 Flashes^a

fit	S ₋₁ (%)	S ₋₂ (%)	S ₋₃ (%)	S ₋₄ (%)	S ₋₅ (%)	α (%)	β (%)	d	f _q	Δf _q (%)
a	0.0	100	—	—	—	23.7	4.4	1.009	0.0132	—
b	7.5	20.0	72.5	—	—	11.9	6.1	1.002	0.0044	67
c	9.0	23.0	44.0	13.5	10.5	(7.4)	(2.1)	0.992	0.0014	68
d	9.0	23.0	44.0	13.5	10.5	7.6	2.1	0.992	0.0018	-29

^a Parameters and other symbols as in Tables 1 and 2. Fits: 3a (7 free parameters: S₁–S₋₂, α, β, d), S₋₁ and S₋₂, the miss and double-hit probabilities, and the activity parameter d were optimized; 3b (8 free parameters), as 3a, but in addition the S₋₃ state population was adjusted; 3c (8 free parameters), the miss and double-hit probabilities were fixed to the values obtained for the control pattern (see Table 1) and the initial S₋₄ and S₋₅ populations were freely adjusted; and 3d (10 free parameters), as last fit, but also the miss and double-hit probabilities were free parameters. The relative change in the fit quality (Δf_q) is always calculated with respect to the previous fit.

and the other rates have been adjusted according to given ratios. This assumption is based on previous results on the rate constants for the reduction rates of redox states S₀–S₃ (Messinger et al., 1991b). An estimate obtained from the decay of Y₅ in Figure 3A was used for the very slow reduction of S₋₁ (see Table 2 for details). No automatic fit routine was used, but the parameters were varied manually according to different fit strategies outlined below.

Although the extended Kok model contains 13 parameters (9 initial S_i state populations, α, β, d, and k_{2,0}), usually only 8 or less free parameters were used (see Tables 1–4). This was achieved as follows. (a) The initial S₃ and S₂ populations were set to zero. (b) k_{2,0} is used only in fits where S₋₄ and S₋₅ were excluded (set to zero). (c) In fits including S₋₄ and S₋₅, α and β were fixed to the values determined in the control pattern. Point (a) is justified, as the initial S₃

Table 4: Fit Results for Oxygen Oscillation Patterns Measured after Different Dark Incubation Times of Spinach S_1 Thylakoids with 10 mM NH_2NH_2 Using Two Different Fit Approaches within the Extended Kok Model^a

incubation time (min)	$k_{2,0}$ (s^{-1})	S_1 (%)	S_0 (%)	S_{-1} (%)	S_{-2} (%)	S_{-3} (%)	S_{-4} (%)	S_{-5} (%)	d	f_q
1	(0.50)	8.0	0.0	92.0	0.0	0.0	—	—	1.000	0.0439
5	(0.50)	2.0	0.0	98.0	0.0	0.0	—	—	1.015	0.0296
10	(0.50)	0.0	0.0	90.0	0.0	10.0	—	—	1.025	0.0132
30	(0.50)	—	—	60.0	5.0	35.0	—	—	1.045	0.0066
60	(0.50)	—	—	29.5	20.5	50.0	—	—	1.030	0.0040
120	(0.50)	—	—	7.5	39.0	53.5	—	—	1.005	0.0067
150	(0.50)	—	—	7.0	47.0	46.0	—	—	1.020	0.0190
1	—	9.5	1.0	75.0	1.0	13.5	0.0	0.0	0.978	0.0052
5	—	1.0	0.5	69.5	3.0	20.0	6.0	0.0	0.980	0.0005
10	—	0.0	0.0	62.0	4.5	25.5	8.0	0.0	0.982	0.0006
30	—	—	—	39.5	8.0	36.0	10.5	6.0	0.994	0.0023
60	—	—	—	20.0	16.5	42.0	14.0	7.5	0.996	0.0005
120	—	—	—	6.5	29.0	43.5	12.5	8.5	1.000	0.0019
150	—	—	—	6.5	34.5	39.5	12.5	7.0	1.000	0.0018

^a The data were simulated with the assumption that either S_{-5} (bottom half of this table) or S_{-3} (top half of this table) is the lowest redox state of the water oxidase. In the latter case (top half of this table), reactions of hydrazine with the S_i states between the flashes were taken into account. The values for misses, double hits, and the rate constants for the two-electron reductions of the S_i states between the flashes were restrained to the values found in the corresponding fits of the pattern obtained after 90 min of incubation with 10 mM NH_2NH_2 (see Table 2, fits 2d and 2e).

and S_2 state populations were determined independently from the control patterns taken immediately before the start of the dark incubation with the reductant hydrazine. These measurements show no S_3 and S_2 state populations, except for a very small apparent S_2 population due to a higher double-hit probability in the first flash (see below).

In many fits, the actual number of parameters varied was 5 or 6 because no oxygen yields were observed before the 5th flash, and therefore, the S_1 and S_0 state populations could also be set to zero. However, S_1 and S_0 have always been counted as free parameters for the calculation of the fit quality (f_q), as Y_3 and Y_4 were necessary for this determination. In order to keep the activity parameter d as constant as possible between the different fits (and close to 1.0), in general, only the first 10 flashes of the flash train were analyzed. The latter point is important, as a value for d that is too small can generate the “need” to introduce initial S_i state populations of S_i states below S_1 . In addition, fits on the full sequence (16 flashes) are shown for the pattern measured after 90 min of incubation of S_1 thylakoids with 10 mM hydrazine (Table 3). For this pattern, d values close to 1.0 were obtained using all 16 flash yields for the fits, because of the relative increase in the electron acceptor pool size discussed above.

In Table 1, different fits for the dark-adapted control sample (Figure 1A) are presented using the extended Kok model. Although the traditional approach using only S_1 (set here to 100%) and the miss and double-hit probabilities leads to a largely satisfactory fit (fit 1a), significant improvements of the fit quality can be achieved by including further parameters like the activity parameter (fit 1b) and a small fraction (approximately 3–4%) of the S_{-1} state population (fit 1c) and by considering a small percentage of the apparent S_2 state population (1.5–2.5%, fit 1d). In contrast, no improvement of the fit quality could be achieved by including S_0 (fit 1e) or the further reduced states S_{-2} – S_{-5} (not shown). To show the reproducibility of measurements and fits, the fit results of two other independent measurements of the same sample are shown in Table 1 (fits 1f and 1g). The small apparent S_2 population in these long dark-adapted samples can be explained by a higher double-hit probability in the first flash owing to a small fraction of oxidized non-heme

iron at the acceptor site (Jursinic, 1981). At first glance, the small S_{-1} population might, however, be a surprising finding, as it is generally accepted that in the absence of exogenous reductants S_1 and S_0 are the only dark stable states of the WOC. Interestingly, much higher S_{-1} populations were reported earlier for dark-adapted algae (Bader et al., 1983; Meunier et al., 1996) and especially in mutants either lacking the extrinsic 33 kDa protein (Burnap et al., 1992; Engels et al., 1994) or having a modified CP47 protein (Gleiter et al., 1994, 1995). The possibility that a similar effect occurs to a lesser extent in intact thylakoids cannot therefore be excluded, as we find small discrepancies between the oxygen yield in the 5th flash and the respective fits consistently for long term dark-adapted samples (unpublished results), if we do not include S_{-1} as a parameter. In principle, another explanation for this finding could be that the S_{-1} population found here is truly a fraction of centers in the state S_0Y_D , which back-react to $S_1Y_D^{ox}$ during the flash train. However, under our measuring conditions (10 °C and pH 6.8), the rates for S_2 reduction by Y_D are slow compared to the flash frequency of 2 Hz [see Messinger and Renger (1993)] so that the presence of Y_D leads to a small increase in the miss probability rather than to an apparent S_{-1} population. This is demonstrated by fit 1h which was obtained from a sample in which all Y_D was oxidized by the preillumination with one flash and a subsequent dark adaptation for 2 h on ice before the measurement. Here, almost identical S_i state populations were found, and only the miss probability decreased from about 7.4 to 6.9%. Independent of the question about the true origin of the small apparent S_{-1} populations in the control samples, which is beyond the scope of this paper, these results demonstrate that excellent fits of the controls are achieved without including any further reduced states like S_{-2} – S_{-5} and that therefore possible systematic errors during the determination of the S_i state populations in the hydrazine incubated samples are likely to be small.

As expected from the qualitative analysis of the oxygen oscillation patterns, it is impossible to fit all the data obtained after hydrazine incubation in this study consistently by assuming that the S_{-2} state is the lowest oxidation state of the water oxidase. For example, in this case neither an

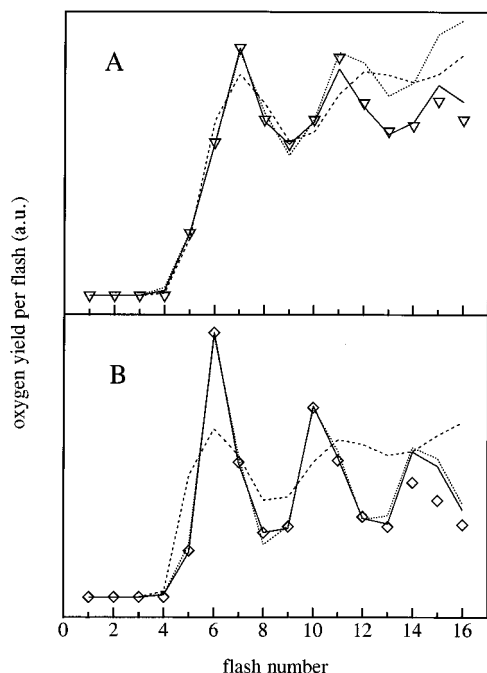


FIGURE 5: Comparison of the oxygen oscillation patterns obtained through a 90 min dark incubation of S₁ thylakoids (A, inverted triangles) or S₀ thylakoids (B, diamonds) on ice in the presence of 10 mM NH₂NH₂ with fits using the extended Kok model (see Materials and Methods) under different sets of restraints: broken lines (fit 2c, seven free parameters, S₁–S₋₂, α , β , d), best fits assuming that S₋₂ is the lowest oxidation state of the water oxidase [for the fit in panel B, the same miss and double-hit probabilities and the same d factor were used as determined in panel A and only the S_i states were varied accordingly (fit 2f, four free parameters)]; dotted lines (eight free parameters), as before, but assuming that S₋₃ is the lowest oxidation state (fits 2c and 2g); solid lines (eight free parameters), the miss and double-hit parameters were fixed to those found in the control sample (see Table 1), but all the S_i state populations were optimized assuming that S₋₅ is the lowest redox state of the water oxidase (fits 2e and 2i). In all cases, only the oxygen yields of the first 10 flashes were used for the fits. For further details about the fit parameters and the fit qualities, see Table 2.

increased miss parameter (Table 2, fits 2b and 2f; broken lines in Figure 5A,B) nor the inclusion of fast hydrazine reduction reactions of the S_i states in the dark time between the flashes (fit 2j and broken line in Figure 6A) leads to acceptable fits.

The inclusion of S₋₃ as an additional parameter improves the fits markedly (by about 80% for the 10-flash fits and about 70% for the 16-flash fit; see Tables 2 and 3 and compare the broken and dotted lines in Figure 5A,B), but different miss and double-hit probabilities have to be used for samples with a high S₋₃ population compared to those with a high S₋₂ population (see fits 2c and 2g). Furthermore, activity parameters exceeding $d = 1.000$, which correspond to an increase of the number of active centers during the flash train (photoactivation), had to be used in the case of high S₋₃ populations (Figure 5A, dots and fit 2c). A similar phenomenon was recently observed in thylakoid samples treated with hydrazine at different pH values (Kekebus et al., 1995) and was thoroughly analyzed in PsbO deletion mutants of cyanobacteria (Engels et al., 1994) and in CP47 mutants of *Synechocystis* PCC6803 (Gleiter et al., 1994, 1995). However, an inspection of the data and fits depicted in Figure 5A,B reveals that the introduction of an activity parameter d of >1.000 does not provide an adequate

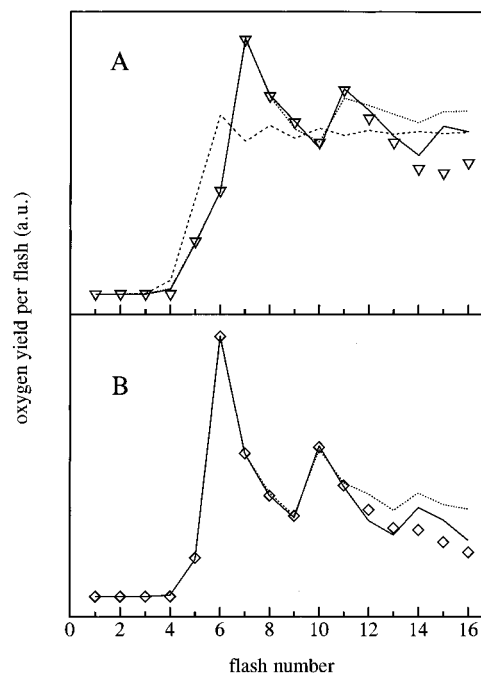


FIGURE 6: Comparison of oxygen oscillation patterns of spinach thylakoids with fits calculated with the extended Kok model under different sets of assumptions. The patterns were measured after 10 min of incubation of S₁ thylakoids with 100 mM NH₂NH₂ on ice (A, inverted triangles) or after 1 min of incubation of S₁ thylakoids with 100 mM NH₂NH₂ plus one flash plus a further 10 min incubation on ice (B, diamonds). The first 10 flash yields were used for all the fits. Dotted lines (fits 2k and 2m, eight free parameters, S₁–S₋₃, α , d , $k_{2,0}$): S₋₃ is the lowest oxidation state, but reactions of hydrazine with the S₃–S₋₁ states in the dark time of 500 ms between the flashes were taken into account. The rate constants for these reactions have been kept at a fixed ratio as determined in previous experiments (see Table 2). In addition, the double-hit parameter β was set to the value of the controls (Table 1). Broken line (fit 2k, six free parameters): as above, but S₋₂ was assumed to be the lowest oxidation state. The miss parameter α was kept to the value determined in the above fit. Solid lines (eight free parameters): no reactions between the flashes, but S₋₅ is assumed to be the lowest redox state of the water oxidase. Misses and double hits are kept in this case to the same values as determined for the controls (Table 1). For further details, see Table 2 and the text.

description of the data obtained in this study, as especially at higher flash numbers large deviations are observed. In this respect, it is also worth mentioning that the quantum yield found in photoactivation experiments is usually very small; i.e. several hundred flashes are necessary for this process to occur [see e.g. Ananyev and Dismukes (1996)] compared to only 16 flashes used here.

The solid lines in Figures 5 and 6 represent simulations that additionally include the formal redox states S₋₄ and S₋₅ as fit parameters. In order to restrict the number of free parameters to 8, for these fits, the miss and double-hit probabilities were fixed to values determined for the control patterns (see Table 1). Excellent results are obtained for all patterns with further improvements of the fit quality by 86 and 68% for the 10-flash fits (Table 2) and 16-flash fits (Table 3), respectively. Normalized S₋₃ populations of almost 50% were determined under these conditions (fit 2l and Figure 6). The maximal apparent S₋₄ and S₋₅ populations were found to be 21% (S₋₄, fit 2h) and 17.5% (S₋₅, fit 2l), respectively. Using all 16 flashes, the approach of fixing the miss and double-hit parameters to the values of the control was checked. The comparison of fits 3c and 3d

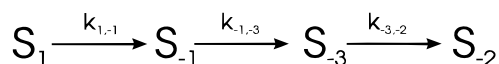
shows that no improvement of the fit quality can be achieved by additionally varying these parameters.

Since the qualitative analysis seemed to exclude a systematic S_{-4} and S_{-5} formation (marked shifts of the oxygen yield toward Y_8 and Y_9 were not observed), fitting of the data was attempted without S_{-4} and S_{-5} by assuming fast reduction reactions of the higher S_i states, especially of S_2 , with hydrazine during the dark time between the flashes. Very good fits could be achieved for the patterns obtained after 100 mM hydrazine incubation using for both simulations (fits 2k and 2m; Figure 6, dotted lines) identical rate constants for the presumed hydrazine-induced reactions $S_3 \rightarrow S_1$, $S_2 \rightarrow S_0$, $S_1 \rightarrow S_{-1}$, $S_0 \rightarrow S_{-2}$, and $S_{-1} \rightarrow S_{-3}$. The value found for $k_{2,0}$ (Table 2) is well in the range that might be expected assuming that part of the hydrazine has diffused from the sample through the dialysis membrane into the flow buffer during the 30 s dark time on the Joliot type electrode before the measurement.

Similar fits were performed for the data obtained by the incubation of thylakoids with 10 mM hydrazine. Because of the linear dependency of the rate constants for S_i state reduction by hydrazine (Messinger et al., 1991b), rate constants 10 times smaller compared to those of 100 mM hydrazine should be expected to yield good results. This is not the case, and identical rate constants or rate constants only about 3–4 times smaller were found to give acceptable fits for the data at 10 mM hydrazine (Table 2). It was also not possible to fit the data with high S_{-3} (fit 2d) and S_{-2} (fit 2h) using the same set of rate constants for the S_i state reductions between the flashes. In addition, Table 4 (top half) shows that with this fit approach f_q varies strongly with the incubation time, if for all patterns the same set of rate constants was used as determined in fit 2d. In contrast, only a comparatively small variation of f_q is observed if S_{-4} and S_{-5} are used as free parameters (Table 4, bottom half and fit 2e). We, therefore, conclude that it is necessary to include the formal redox states S_{-4} and S_{-5} in the fits in order to obtain consistent results.

Calculation of the Rate Constants for Hydrazine-Induced S_{-1} Reduction to S_{-3} and for the Oxidation of S_{-3} to S_{-2} . Figures 7 and 8 display the calculated normalized S_{-1} – S_{-3} state populations (top, A) and formal S_{-4} and S_{-5} populations (bottom, B) as a function of the dark incubation time of S_1 thylakoids with 10 and 100 mM hydrazine, respectively. For the sake of clarity, the rapid decay of the initial S_1 state population is not shown. With the exception of some deviations at short incubation times, the time course of the S_{-1} , S_{-3} , and S_{-2} formation can be satisfactorily simulated by the sequence of simple first-order reactions shown in Scheme 1:

Scheme 1



The first-order rate constants used for the fits, which are represented by solid lines in Figures 7A and 8A, are given in Table 5. Depending on the hydrazine concentration, about 75% (10 mM) or 55% (100 mM) of the initial S_1 state population seems to follow this reaction path. The fairly good agreement of the fits with the time course of the S_{-1} , S_{-3} , and S_{-2} populations, together with the fact that the rates found for S_1 and S_{-1} reduction were, as should be expected,

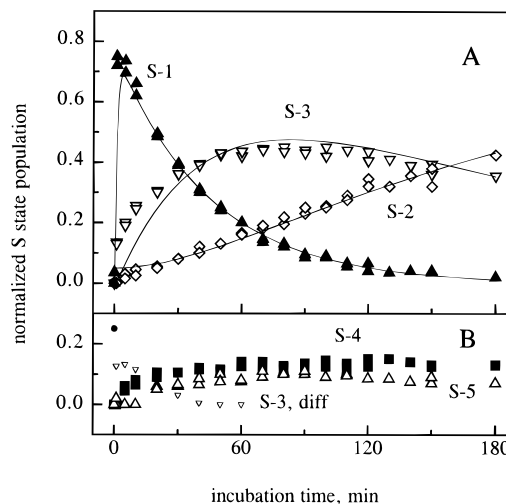


FIGURE 7: Normalized S_i state populations of spinach thylakoids as a function of dark incubation time with 10 mM NH_2NH_2 . The measurements shown in Figure 3A were deconvoluted assuming that S_{-5} is the lowest redox state of the water oxidase. Misses and double hits were kept at the values determined for the control. The results of two independent measurements are shown. Lines display kinetic fits according to Scheme 1. The rate constants used are given in Table 5. For the sake of clarity, the fast-decaying S_1 population is not shown. The S_{-1} – S_{-3} populations are shown in the top of this figure (A), while panel B displays the formal S_{-4} and S_{-5} populations along with the difference between the simulated (Scheme 1) and calculated (extended Kok model) S_{-3} population (S_{-3} , diff).

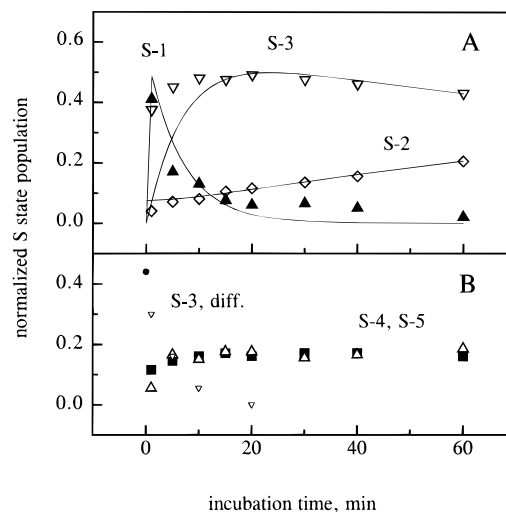


FIGURE 8: Normalized S_i state population of spinach thylakoids as a function of dark incubation time with 100 mM NH_2NH_2 . The measurements shown in Figure 4A were deconvoluted assuming that S_{-5} is the lowest redox state of the water oxidase. Misses and double hits were kept at the values determined for the control. Lines display kinetic fits according to Scheme 1. The rate constants used are given in Table 5. For the sake of clarity, the fast-decaying S_1 population is not shown. The S_{-1} – S_{-3} populations are shown in the top of this figure (A), while panel B displays the formal S_{-4} and S_{-5} populations along with the difference between the simulated (Scheme 1) and calculated (extended Kok model) S_{-3} population (S_{-3} , diff).

about 7–10 times higher with 100 mM hydrazine than with 10 mM hydrazine, suggests that the formation of the formal S_{-4} and S_{-5} states occurs through a mechanism that is different from the reaction path leading to the S_{-3} formation. This interpretation is supported by the very rapid formation of some S_{-3} population which cannot be accounted for by the linear reaction sequence shown in Scheme 1. This

Table 5: Rate Constants for the Two-Electron Reduction of the S₁ and S₋₁ State by NH₂NH₂ and for the Univalent Oxidation of the S₋₃ to the S₋₂ State in Spinach Thylakoids at 0 °C and pH 6.8^a

	centers following Scheme 1 (%)	$k_{1,-1}$	$k_{-1,-3}$	$k_{-3,-2}$
10 mM NH ₂ NH ₂	75	1.0 min ⁻¹	0.0225 min ⁻¹	0.0055 min ⁻¹
100 mM NH ₂ NH ₂	56	(~10.0 min ⁻¹)	0.1500 min ⁻¹	0.0050 min ⁻¹
ratio (k_{100}/k_{10})	—	~10.0	6.7	0.9
average rate	—	1.7 M ⁻¹ s ⁻¹	0.032 M ⁻¹ s ⁻¹	8.8 × 10 ⁻⁵ s ⁻¹

^a The rate constants were obtained from the simulation of the incubation time dependence of the S_i state populations in the presence of 10 mM (Figure 7A) and 100 mM (Figure 8A) hydrazine.

difference between the fitted S₋₃ population (lines) and the S₋₃ population extracted with the extended Kok model from the individual flash pattern (inverted triangles, Figures 7A and 8A) is shown in the bottom parts (B) of Figures 7 and 8 as small inverted triangles (S_{-3, diff}) along with the formal S₋₄ (squares) and S₋₅ (triangles) populations. Qualitatively, the time course of S_{-3, diff} seems to follow that of the S₋₁ population, and those of S₋₄ and S₋₅ seem to follow that of the S₋₃ population. No attempts were made to simulate these time courses. The possible nature of the formal S₋₄ and S₋₅ states is discussed below.

DISCUSSION

Properties of the S₋₃ State. The data presented in this paper provide direct evidence for the existence of a discrete and relatively stable S₋₃ state. The rate of its hydrazine-induced formation from S₋₁ is about 50 times slower than the reduction of S₁ to S₋₁. For this reason and because of its reoxidation to S₋₂ ($t_{1/2}$ = 130 min at pH 6.8 and 0 °C), the redox state S₋₃ escaped an unambiguous detection in previous studies. It is interesting to note that the S₋₃ state can apparently also be reached by incubation of chloroplasts with hydroxylamine. A quantitative analysis of the data presented by Bouges (1971, Figure 3, trace 5) with the extended Kok model used in this study gives approximately the following S_i state distribution: [S₋₁] = 10%, [S₋₂] = 60%, and [S₋₃] = 30% [see also the discussion in Laverne (1989)].

As found earlier for the flash-induced transitions S₋₂ → S₋₁ and S₋₁ → S₀ (Messinger et al., 1991b), the reaction S₋₃Y_Z^{ox} → S₋₂Y_Z does seem to occur with about the same efficiency as the normal S_i state transitions, as no evidence could be found for an increased miss parameter coupled to that transition. This indicates two things about the S₋₃ state. (i) The manganese ions of the PS II centers that remain active in O₂ evolution are still in their original binding sites, and (ii) centers that are inactivated are not easily photoactivated during the flash sequence. This is important as one could imagine a situation in which the reduction of the WOC leads to Mn(II) ions that are released from their original binding sites [possibly due to the loss of the μ-oxo bridges of the dimers (Riggs-Gelasco et al., 1996)] but remain bound to the protein matrix. In this case, the restoration of the WOC could occur with a quantum yield significantly higher than that in the normal photoactivation process and an O₂ oscillation pattern that is formally described by a higher miss parameter than that of the normal WOC turnover could arise.

The well-known inactivation of PS II in the presence of hydrazine or hydroxylamine is coupled with the release of Mn²⁺, and it has been speculated that it occurs via a very unstable S₋₃ state (Beck & Brudvig, 1987). This proposal was based on the fact that Mn(II), which can be expected to

be formed during the S₋₃ formation (see below), has a lower ligand field stabilization energy and is therefore expected to be less tightly bound by the water oxidase. The results of this study show that it is possible to stabilize the S₋₃ state under suitable conditions to an extent that it is practically as stable as the S₋₂ and S₋₁ states. This is supported by the fits of the time courses of the S₋₁, S₋₃, and S₋₂ populations according to Scheme 1 (see Figures 7 and 8), which would not be possible if the S₋₃ state is significantly less stable within the time domain of the experiment than the other S_i states. The inactivation of oxygen evolution appears therefore to occur largely independent of the redox state of the water oxidase and may be rate limited by reactions of hydrazine with the protein matrix or with other cofactors of PS II.

Dark Oxidation of S₋₃ to S₋₂. Hydrazine can, in principle, react either as a reductant or as an oxidant toward the water oxidase, as it is known for example for hydrogen peroxide (Velthuys & Kok, 1978; Mano et al., 1987; Frasch & Mei, 1987). It is, therefore, interesting that the rate constant $k_{-3,-2}$ for the S₋₃ → S₋₂ transition was found to be independent of the hydrazine concentration (see Table 5). This suggests that this reaction involves either another exogenous oxidant like dissolved oxygen or an endogenous electron acceptor of PS II. In a previous report, the S₋₁ and S₋₂ states were shown to be oxidized by Y_D^{ox} at rates that are comparable to the well-established S₀ oxidation (Messinger & Renger, 1993). It is, therefore, tempting to speculate that the S₋₃ oxidation to S₋₂ occurs via the same mechanism, especially as the half-time of this reaction is only about 4 times slower than that of the transition S₀Y_D^{ox} → S₁Y_D at 0 °C (Messinger et al., 1993). Another endogenous one-electron acceptor could be for example cytb₅₅₉ in its low-potential form. Further experiments are required to clarify this point.

Possible Electronic Configuration of the S₋₃ State. It is now widely accepted that the two-electron reduction of S₁ to S₋₁ is a metal (manganese)-centered process (see the introductory section). Therefore, two different possibilities have to be considered for the electronic configuration of S₋₃. (1) The WOC attains a redox level that is 4 equiv below S₁. (2) The WOC is reduced to S₋₁ (S₋₂), and the additional reducing equivalents are provided by bound NH₂NH₂ (NH₂OH). For the following reasons, S₋₃ is assumed to be a super-reduced state of the WOC: (1) the overall similarities between the hydrazine-induced reactions S₁ → S₋₁ (Messinger et al., 1991b) and S₋₁ → S₋₃ (this report), i.e. the clear two-electron shifts without a significant rise of the miss parameter in both cases (see also the discussion on S₋₄ and S₋₅), and (2) the slow rate of dark formation of S₋₃.

On the basis of the first point, i.e. the clear two-electron shift and the unchanged Kok parameters, it is reasonable to assign the S₋₃ formation to the reduction of the manganese

ions of the water oxidase rather than to a reduction of a protein component in its vicinity. For example, the possibility that the S_{-3} state equals $S_{-2}Y_D$ can be excluded for kinetic reasons, as the reduction of S_2 by Y_D is slow under the experimental conditions compared to the flash frequency of 2 Hz. Therefore, only a minor shift in the oxygen yields can be observed upon the reduction of Y_D^{ox} to Y_D , which can be best described by an increase in the miss parameter rather than an S_i state reduction [see Figures 2g and 4g in Messinger and Renger (1993)]. If one additionally accepts that this complex contains four manganese atoms [for reviews, see Debus (1992), Rutherford et al. (1992), and Renger (1993); a value of six manganese atoms reported by Pauly and Witt (1992) has not been confirmed by other groups] and that Mn(II) is the lowest possible redox state, the following electronic configurations have to be considered for the manganese cluster in redox state S_{-3} :

WOX	C	WOX	C
a Mn(II)Mn(II)	Mn(II)Mn(II)		
b Mn(II)Mn(II)	Mn(III)Mn(III) or Mn(III)Mn(II)	Mn(II)Mn(II)	
c Mn(II)Mn(III)	Mn(II)Mn(III)		
d Mn(II)Mn(II)	Mn(II)Mn(IV) or Mn(II)Mn(IV)	Mn(II)Mn(II)	

where WOX (water oxidase) and C refer to the two bis- μ -oxo bridged manganese dimers which are assumed to have different functional properties in the mechanism of water oxidation (Renger, 1987) and reactivities toward exogenous reductants (Messinger & Renger, 1993). Similarly, Riggs-Gelasco et al. (1996) are distinguishing between a low-potential dimer (site A) and a high-potential dimer (site B). It should also be kept in mind that the individual manganese ions within each dimer may have different redox potentials due to their specific protein ligation.

The stability of the S_{-3} state under the conditions of this study (see above) favors configurations **b** [see also Riggs-Gelasco et al. (1996)], **c**, or **d** over configuration **a**, as they still contain higher-valent manganese ions. For a definitive assignment of the redox states of the manganese cluster, it would be very important to know if the formal redox states S_{-4} and S_{-5} found in this study represent additional manganese redox states of the water oxidase or are due to other effects of this exogenous reductant.

Formal Redox States S_{-4} and S_{-5} . In contrast to the S_{-3} formation, the formal redox states S_{-4} and S_{-5} do not arise from a straightforward two-electron reduction from S_{-2} and S_{-3} , respectively, and seem to occur only in a fraction of the PS II centers. The amount of S_{-4} and S_{-5} formation is not linearly dependent on the hydrazine concentration and, after a relatively short transient period, is basically independent of the incubation time. The most likely possibility for this phenomenon seems, therefore, to be that there is a low-affinity binding site for hydrazine near the manganese cluster. In this case, high hydrazine concentrations would lead to the binding of hydrazine molecules to a fraction of the water oxidases. The hydrazine molecule could then act as a donor of one or two electrons during the flash sequence and thereby explain the almost parallel appearance of $S_{-3, diff}$ (and some S_{-2}) with S_{-1} and also the similar rise of the S_{-4} and S_{-5} population with that of S_{-3} . Two different sites of amine binding to the water oxidase have been previously reported for the case of ammonia [for review, see Rutherford et al. (1992)], and the same might be true for hydroxylamine (Mei & Yocum, 1993). If this scenario were true, then possibility

a, i.e. four Mn(II) in the S_{-3} state and therefore four Mn(III) in S_1 , would become a possibility for the manganese ions in the water oxidase.

However, alternative explanations cannot be excluded. It is conceivable for example that it is very difficult to reduce one Mn(IV) or two Mn(III) ions of the water oxidase in structurally intact systems but that it would become a relatively fast reaction in slightly modified PS II complexes. Such a modification could comprise a less tight binding or even temporary loss of certain extrinsic proteins into the lumen during the mixing process of the highly concentrated hydrazine stock solution with the thylakoids at the start of the reaction. Another possibility is that the order of reduction of the different manganese ions in the water oxidase may be important for reaching the S_{-4} and S_{-5} states (e.g. in case of possibility **c**, it may be difficult for a two-electron donor like hydrazine to reduce the S_{-3} state).

CONCLUSIONS

Although on the basis of oxygen oscillation pattern alone it is practically impossible to definitively rule out the scenarios in which one or two reducing equivalents of the S_{-3} state are not stored on the manganese cluster itself, a higher miss parameter and/or different rates of hydrazine-induced S_{-3} formation from S_{-1} or reoxidation rates to S_{-2} should be expected for those cases. Therefore, we strongly favor the idea that the S_{-3} formation involves, just like the S_{-1} formation, a reduction of the manganese cluster by hydrazine.

In contrast, no clear assignment can be given at the present time for the nature of formal redox states S_{-4} and S_{-5} , because of their different rates of formation and the low population levels that are achieved in this study. Therefore, our present data support the idea that the minimum average oxidation state of the four Mn ions of the water oxidase is Mn(III), but do not permit a distinction between models that suggest an electronic configuration of four Mn(III) in S_1 (Zheng & Dismukes, 1996) and those that favor two Mn(III) and two Mn(IV) (Riggs-Gelasco et al., 1996; Roelofs et al., 1996).

ACKNOWLEDGMENT

J. Messinger thanks Prof. C. B. Osmond and Prof. M. C. W. Evans for their support. He also thanks Prof. M. C. W. Evans, Dr. J. H. A. Nugent, and Dr. S. Turconi for helpful discussions and critically reading the manuscript.

REFERENCES

- Ananyev, G. M., & Dismukes, G. C. (1996) *Biochemistry* 35, 4102–4109.
- Bader, K. P., Thibault, P., & Schmid, G. H. (1983) *Z. Naturforsch.* 38C, 778–792.
- Beck, W. F., & Brudvig, G. W. (1987) *Biochemistry* 26, 8285–8295.
- Bouges, B. (1971) *Biochim. Biophys. Acta* 234, 103–112.
- Brudvig, G. W., & Beck, W. F. (1992) in *Manganese Redox Enzymes* (Pecoraro, V. L., Ed.) pp 119–140, VCH Publishers, Inc., New York.
- Burnap, R. L., Shen, J. R., Jursinic, P. A., Inoue, Y., & Sherman, L. A. (1992) *Biochemistry* 31, 7404–7410.
- Debus, R. J. (1992) *Biochim. Biophys. Acta* 1102, 269–352.
- Delrieu, M.-J., & Rosengard, F. (1987) *Biochim. Biophys. Acta* 892, 163–171.

- Engels, D. H., Lott, A., Schmid, G. H., & Pistorius, E. K. (1994) *Photosynth. Res.* 42, 227–244.
- Frasch, W., & Mei, R. (1987) *Biochemistry* 26, 7321–7325.
- Gleiter, H. M., Haag, E., Shen, J.-R., Eaton-Rye, J. J., Inoue, Y., Vermaas, W. J. F., & Renger, G. (1994) *Biochemistry* 33, 12063–12071.
- Gleiter, H. M., Haag, E., Shen, J.-R., Eaton-Rye, J. J., Seeliger, A., Inoue, Y., Vermaas, W. J. F., & Renger, G. (1995) *Biochemistry* 34, 6847–6856.
- Guiles, R. D., Yachandra, V. K., McDermott, A. E., Cole, J. L., Dexheimer, S. L., Britt, R. D., Sauer, K., & Klein, M. P. (1990) *Biochemistry* 29, 486–496.
- Hansson, Ö., & Wydrzynski, T. (1990) *Photosynth. Res.* 23, 131–162.
- Joliot, P. (1972) *Methods Enzymol.* 24B, 123–134.
- Joliot, P., Barbieri, G., & Chabaud, R. (1969) *Photochem. Photobiol.* 10, 309–329.
- Jursinic, P. (1981) *Biochim. Biophys. Acta* 635, 38–52.
- Kebekus, U., Messinger, J., & Renger, G. (1995) *Biochemistry* 34, 6175–6182.
- Kok, B., Forbush, B., & McGloin, M. (1970) *Photochem. Photobiol.* 11, 457–475.
- Kretschmann, H., & Witt, H. T. (1993) *Biochim. Biophys. Acta* 1144, 331–345.
- Kretschmann, H., Pauly, S., & Witt, H. T. (1991) *Biochim. Biophys. Acta* 1059, 208–214.
- Lavergne, J. (1989) *Photochem. Photobiol.* 50, 235–241.
- Mano, J., Takahashi, M.-a., & Asada, K. (1987) *Biochemistry* 26, 2495–2501.
- Mei, R., & Yocum, C. (1991) *Biochemistry* 30, 7836–7842.
- Mei, R., & Yocum, C. (1993) *Photosynth. Res.* 38, 449–453.
- Messinger, J. (1993) Ph.D. Thesis, TU Berlin, Berlin, Germany.
- Messinger, J., & Renger, G. (1990) *FEBS Lett.* 277, 141–146.
- Messinger, J., & Renger, G. (1993) *Biochemistry* 32, 9379–9386.
- Messinger, J., Pauly, S., & Witt, H. T. (1991a) *Z. Naturforsch.* 46c, 1033–1038.
- Messinger, J., Wacker, U., & Renger, G. (1991b) *Biochemistry* 30, 7852–7862.
- Messinger, J., Schröder, W. P., & Renger, G. (1993) *Biochemistry* 32, 7658–7668.
- Messinger, J., Badger, M., & Wydrzynski, T. (1995a) *Proc. Natl. Acad. Sci. U.S.A.* 92, 3209–3213.
- Messinger, J., Hillier, W., Badger, M., & Wydrzynski, T. (1995b) in *Photosynthesis: from Light to Biosphere* (Mathis, P., Ed.) pp 283–286, Kluwer, Dordrecht, The Netherlands.
- Meunier, P. C., & Popovic, R. (1991) *Photosynth. Res.* 29, 113–115.
- Meunier, P. C., Burnap, R. L., & Sherman, L. A. (1996) *Photosynth. Res.* 47, 61–76.
- Nugent, J. H. A. (1996) *Eur. J. Biochem.* 237, 519–531.
- Ono, T.-a., Noguchi, T., Inoue, Y., Kusunoki, M., Matsushita, T., & Oyanagi, H. (1992) *Science* 258, 1335–1337.
- Pauly, S., & Witt, H. T. (1992) *Biochim. Biophys. Acta* 1099, 211–218.
- Renger, G. (1987) *Photosynthetica* 21, 203–224.
- Renger, G. (1992) in *The Photosystems: Structure, Function and Molecular Biology* (Barber, J., Ed.) pp 45–99, Elsevier, Amsterdam.
- Renger, G. (1993) *Photosynth. Res.* 38, 229–247.
- Renger, G., Messinger, J., & Fromme, R. (1989) *Z. Naturforsch.* 44C, 423–430.
- Renger, G., Messinger, J., & Hanssum, B. (1990) in *Current Research in Photosynthesis* (Baltscheffsky, M., Ed.) Vol. 1, pp 845–848, Kluwer, Dordrecht, The Netherlands.
- Riggs, P. J., Mei, R., Yocum, C. F., & Penner-Hahn, J. E. (1992) *J. Am. Chem. Soc.* 114, 10650–10651.
- Riggs-Gelasco, P. J., Mei, R., Yocum, C. F., & Penner-Hahn, J. E. (1996) *J. Am. Chem. Soc.* 118, 2387–2399.
- Roelofs, T. A., Liang, W., Latimer, M. J., Cinco, R. M., Rempel, A., Andrews, J. C., Sauer, K., Yachandra, V. K., & Klein, M. P. (1996) *Proc. Natl. Acad. Sci. U.S.A.* 93, 3335–3340.
- Rutherford, A. W., Zimmermann, J.-L., & Boussac, A. (1992) in *The Photosystems: Structure, Function and Molecular Biology* (Barber, J., Ed.) pp 179–229, Elsevier Publishers.
- Velthuys, B., & Kok, B. (1978) *Biochim. Biophys. Acta* 502, 211–221.
- Yachandra, V. K., DeRose, V. J., Latimer, M. J., Mukerji, I., Sauer, K., & Klein, M. P. (1993) *Science* 260, 675–679.
- Zheng, M., & Dismukes, G. C. (1996) *Inorg. Chem.* 35, 3307–3319.

BI962653R